

Some critical aspects of fatigue crack propagation in metallic materials

Jean Petit

LMPM, UMR CNRS 6617, ENSMA, 86961 Chasseneuil-Futuroscope, France

jean.petit@lmpm.ensma.fr

Keywords: fatigue crack propagation, threshold, metallic alloys, microstructure, environment, crack closure.

Abstract. This paper proposes an overview on some critical aspects of fatigue crack propagation in metallic materials; it is mainly concentrated on the near-threshold domain and deals the role of some predominant influencing parameters including intrinsic parameters as the alloy composition and microstructure, or extrinsic factors as loading condition, crack geometry, crack closure, atmosphere environment. The first part is devoted to basic mechanisms of fatigue crack propagation in relation with the alloy microstructure, with the presentation of a framework describing the different intrinsic propagation stages in absence of interaction with environment and crack closure. In the second section, this framework is extended to the environmentally assisted crack propagation in gaseous atmosphere. In the third section, this basic framework is used to analyze some critical examples of crack propagation including small cracks, propagation at low temperature and ultra-slow crack propagation.

Introduction

Defect tolerance design approach to fatigue is based on the premise that engineering structures are inherently flawed. The useful fatigue life then is the number of cycles to propagate a dominant flaw of an assumed or measured initial size (which can be the largest undetected crack size estimated from the sensitivity of non-destructive inspection methods) to a critical dimension which may be dictated by the fracture toughness, limit load, allowable strain or allowable compliance change. In most metallic materials, catastrophic failure is preceded by a substantial amount of stable crack growth under cyclic loading conditions. The propagation rate of these cracks for given loading conditions depends on several factors including crack length and geometry of the cracked structure, crack closure, temperature, environment, test frequency and propagation mechanisms in relation with material microstructure. During the last three decades, the near-threshold Fatigue Crack Propagation (FCP) has been widely investigated. The ability to define the conditions under which cracks or defects are effectively not propagating is a powerful mean in the area of design and failure analysis. The threshold stress intensity factor range, ΔK_{th} , was initially assumed to be a material parameter. However, numerous experimental data showed that ΔK_{th} and near-threshold FCP behavior are dependent on several intrinsic and extrinsic parameters [1- 3].

It has been shown that the number of affecting parameters is reduced by taking into account the contribution of the shielding effect of crack closure [4] Introducing the concept of effective Stress Intensity Factor (SIF) range, ΔK_{eff} , as defined by Elber [4], leads to the concept of effective fatigue threshold and effective fatigue crack propagation which are assumed to be more representative of the intrinsic material properties.

This paper proposes, first, a brief survey of the state of the art on the intrinsic fatigue crack propagation in metallic alloys, which is an essential reference if one intends to uncouple the respective influence of microstructure, closure, and environment. A modeling for environmentally assisted propagation [5, 6] developed on the basis of the framework describing the intrinsic fatigue crack propagation is then presented in a second section of this paper.

The interest in the near-threshold FCP and in the threshold concept has been accentuated by the problem of short fatigue cracks [7-10]. It has been demonstrated that short cracks tend to propagate without closure contribution. An example is given to show that short crack propagation can be described using the framework proposed for effective crack propagation, supporting that the effective threshold and effective propagation behavior emerge as a general concept applicable to many kinds of cracks when requirements for LEFM application are fulfilled.

The fatigue crack propagation behavior of a new generation Al alloy in simulated high atmosphere environment (cold and dry air), is also discussed and analyzed. Finally, ultra slow crack propagation as explored by means of high frequency facilities in air and in vacuum is discussed with an approach for the evaluation of the propagation life of internal cracks.

Basic mechanisms

Intrinsic fatigue crack propagation. Considering that the knowledge of the intrinsic fatigue crack propagation regimes is a fundamental reference when one wants to analyze the role of microstructure, environment and crack closure on fatigue crack growth, a precise characterization of the intrinsic propagation has been undertaken by Petit *et al.*, [5, 6] on the basis of a wide compilation of numerous experimental data obtained on various aluminum alloys (including technical alloys and high purity single crystals), steels and titanium alloys. It has been demonstrated that three intrinsic fatigue crack propagation regimes can be identified as follows:

The intrinsic stage I has been basically identified on single crystals as illustrated in Fig. 1 [11]. However, following the first characterization of stage I cracks by Forsyth [12], stage I has been commonly considered to be typical of the early growth of cracks, with a dominant shear propagation mechanism along a plane inclined at 45° against the load axis. As identified on peak aged Al-Zn-Mg single crystals pre-oriented for single slip (Fig. 1), an intrinsic stage I crack typically develops along a {111} plane inclined at an angle of 45° against the tensile axis with a very flat surface (Fig. 2).

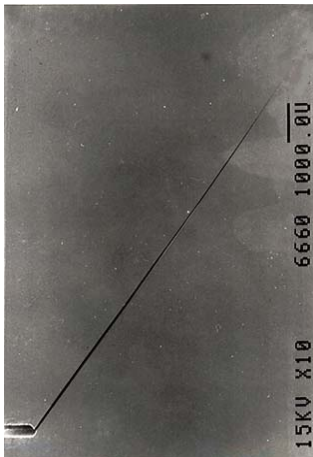


Fig. 1. Stage I crack in peak aged single crystal of Al-4.5% wt Zn-1.25% wt Mg oriented for (111) slip (R=0.1, 35 Hz, high vacuum).

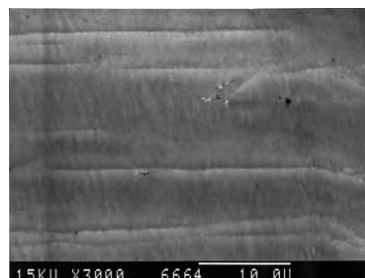


Fig. 2. Fracture surface of the stage I crack of figure 1.



Figure 3. Zig-zag stage I crack grown in high vacuum ($R=-1$ and 35Hz) in an Al-Zn-Mg singlecrystal not oriented for easy slip: a) crack profile with evidences of crack closure, and b) crystallographic crack surface.

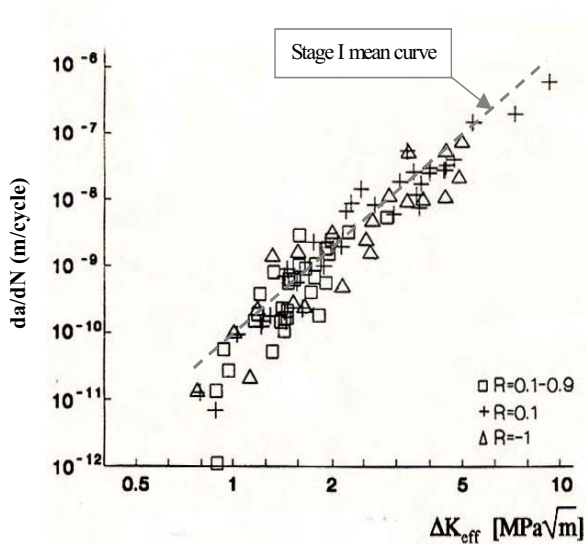


Fig. 4. Intrinsic crack propagation data in high vacuum of single crystals and polycrystals of Al-4.5% wt Zn-1.25% wt Mg alloy with closure corrected ΔK_{eff} for mode I loading ($R=0.1$, 35 Hz).

Such shearing propagation mechanism is favored by the heterogeneous deformation promoted by fine and coherent GP zones; the crack is grown along a persistent slip band which develops within a single slip system. When the crystal (or the grain) is not well oriented for single slip, the crack will find a zigzagging path following (111) planes of different orientations (Fig. 3) and leading to a highly faceted crystallographic crack path. However, after closure correction, the propagation data for pure stage I and zigzagging stage I are comparable (Fig. 4).

The intrinsic stage II is commonly observed on polycrystals and single crystals when crack propagation proceeds on a macroscopic scale along planes normal to the loading direction (examples in Fig. 5).

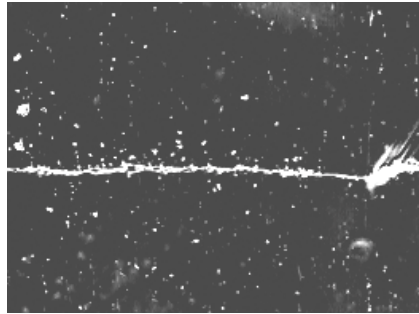


Fig. 5. Intrinsic stage II crack path in overaged polycrystalline Al-4.5% wt Zn-1.25% wt Mg alloy (R=0.1, 35 Hz, high vacuum).

Such propagation is favored by microstructures which promote homogenous deformation and wavy slip, such as small grain size, or large non coherent precipitates in Al alloys [13, 15]. The stage II regime is in accordance with a propagation law proposed by Petit et al. [5, 6, 16] and derived from the models initially proposed by Rice [19] and Weertman [20] :

$$\frac{da}{dN} = \frac{A}{D_0^*} \left(\frac{\Delta K_{eff}}{\mu} \right)^4 \quad (2)$$

where A is a dimensionless constant; μ the shear modulus and D_0^* the critical displacement leading to rupture.

Intrinsic data of well identified stage II for a wide selection of Al alloys, steels and Ti alloys have been shown in very good agreement with the above relation, confirming that the LEFM concept is well adapted to describe the intrinsic growth of a stage II crack (Fig. 6). This regime has been shown to be nearly independent on alloy composition, microstructure (when it does not introduce a change in the deformation mechanism), grain size, and yield stress. The predominant factor is the Young modulus of the matrix, and the slight differences existing between the three base metals can be interpreted as some limited change in the critical cumulated displacement D^* in relation (1) according to the alloy ductility [21].

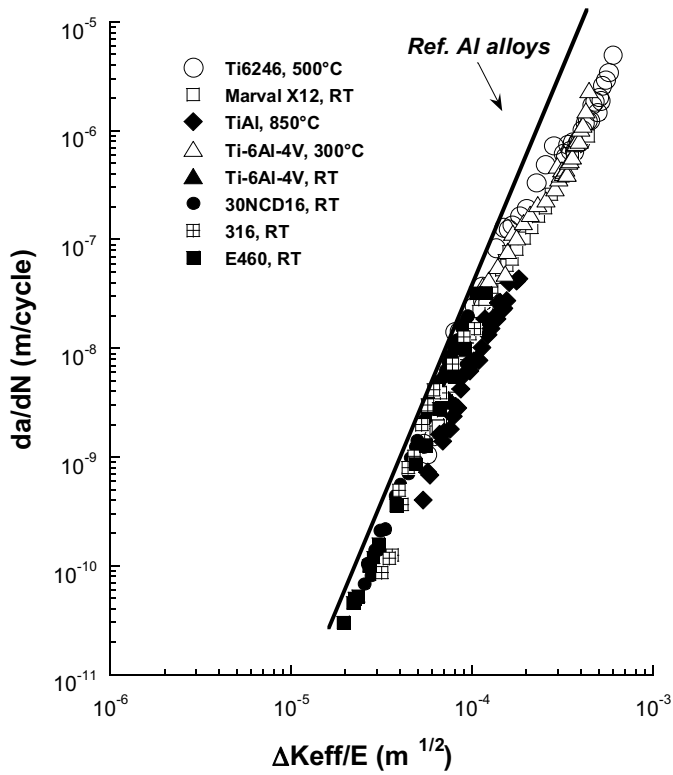


Fig. 6. Intrinsic stage II various steels and Ti alloys (ref. for Al alloys from [19])

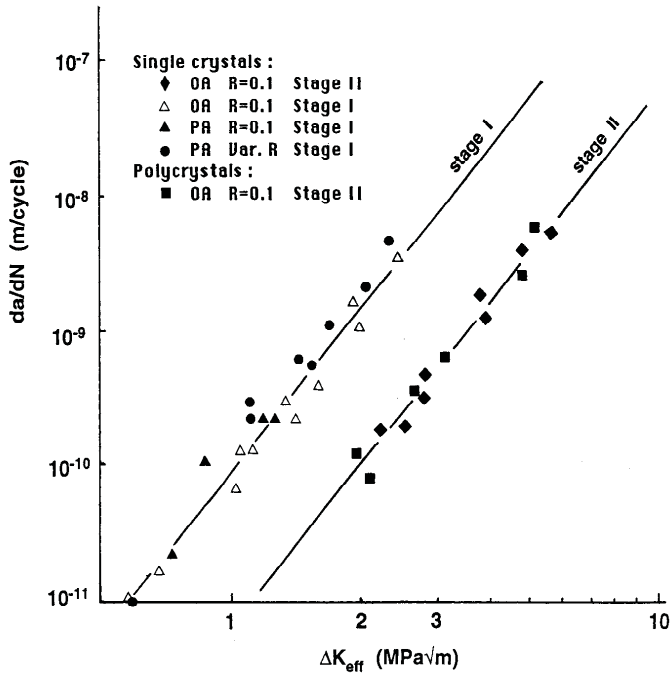


Fig. 7. Intrinsic crack propagation in high vacuum of single and polycrystal of Al-4.5% wt Zn-1.25% wt Mg with ΔK_{eff} as computed for mode I loading (R=0.1, 35 Hz): intrinsic stage I in single crystals is much faster than intrinsic stage II in single crystals and polycrystals [5].

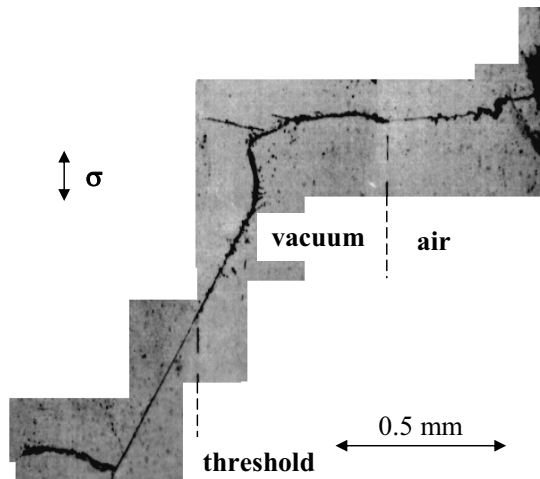


Fig. 8. Intrinsic crack propagation behavior in overaged Al-4.5% wt Zn-1.25% wt Mg single crystal preoriented for easy slip (R=0.1, 35 Hz) [5].

The crack path in a microstructure containing precipitates which can be shared at low ΔK and low rate can also depend on the amplitude of the stress intensity factor at the crack tip. A transition from stage II to stage I (and conversely) has been observed in a overaged single of Al-4.5% wt Zn-1.25% wt Mg alloy preoriented for easy slip and tested in high vacuum (Fig. 8). The initial stage II crack initiated at the notch in the microstructure containing, switches at a critical stress level to a stage I crack grown in the near-threshold domain. After threshold, the stage I crack grown at constant load, thus at increasing ΔK , switches again into the stage II crack when the critical stress level is reached.

The intrinsic stage I-like propagation, generally observed in polycrystal in the near-threshold domain [5, 13, 17, 22] or in the early growth of small cracks [6, 9, 14], is typically associated to a crystallographic crack path. An example of crack profile is given in Fig. 9 for a 7075 Al alloy.

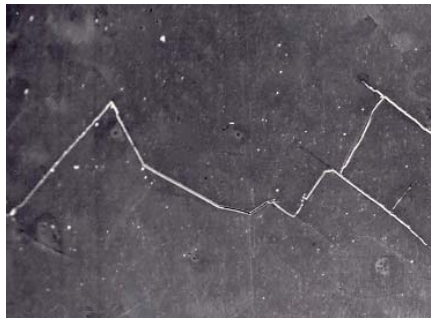


Fig. 9. Intrinsic stage I like crack path in peak-aged polycrystal of Al-4.5% wt Zn-1.25% wt Mg alloy ($R=0.1$, 35 Hz, high vacuum).

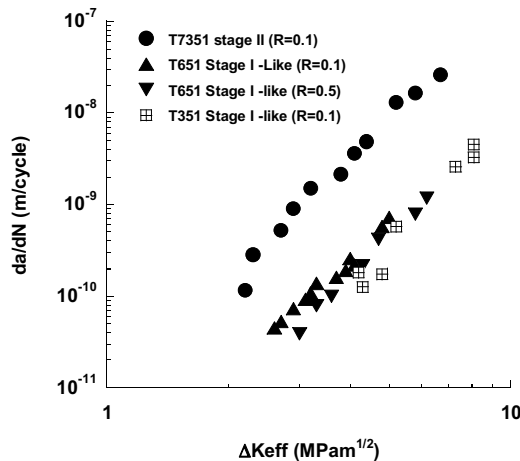


Fig. 10. Comparison of intrinsic stage II and stage I like propagation regimes in a 7175 Aluminum alloy in three different aging conditions tested in high vacuum at 35 Hz.

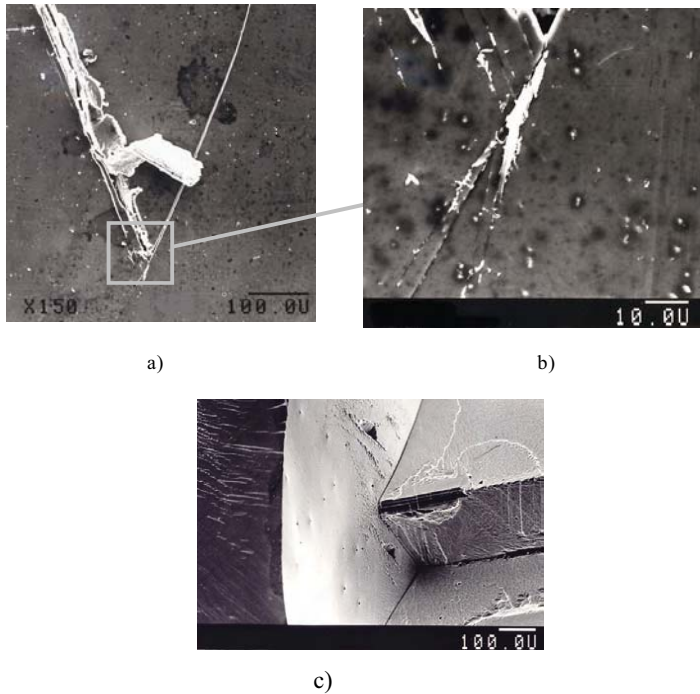


Fig. 11. Barrier effect in Al-Zn-Mg bicrystal: a) grain boundary blockage of a stage I crack; b) initiation of a (111) slip system in the neighbor grain; c) associated fracture surface [22].

In most cases, intrinsic stage I like is much slower than stage II, as shown in Fig. 10 for a 7075 Aluminum alloy in different aged microstructures. The intrinsic stage I-like is prevailing in underaged T351 and peakaged T651 microstructures containing coherent shearable precipitates such as GP zones, while the intrinsic stage II occurs in the overaged microstructure T7351 containing less coherent precipitates [5, 13, 15].

Crack branching or crack deviation mechanisms in single crystals have been shown to induce only small shielding effect on the stress intensity factor at the tip of the main crack (Fig. 4). The strong retardation of the growth rate in the intrinsic stage I-like regime in polycrystals, must be mainly attributed to the barrier effect of grain boundaries [9, 12] which results from the difficulty to generate a new slip system in the next grain as observed in Al-Zn-Mg bicrystal (Fig. 11). In addition, the initiation point of this new slip system is not exactly at the tip of the stage I crack grown in the first grain, and hence a segment of intercrystalline crack path is required to link up the first stage I crack to the new one which develops along one or more (111) planes having other orientations in the next grain (Fig. 11c). In the same manner, a stage I-like crack grown in a polycrystal will meet various grain orientations and finally induce a rough crack path mixing predominant transgranular crystallographic facets and intergranular areas (Fig.12). This barrier effect has also been shown more accentuated when the number of available slip systems is reduced

as in Ti alloys [17] An illustration is given in Fig. 13 for three different microstructure in a Ti-6Al-4V alloys tested at 300°C in high vacuum.

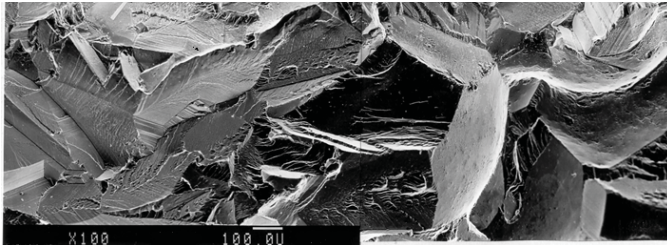


Fig.12. Crack surface of peak-aged Al-Zn-Mg polycrystal with crystallographic (111) facets and intergranular areas (high vacuum, R=0.1 and 35 Hz)

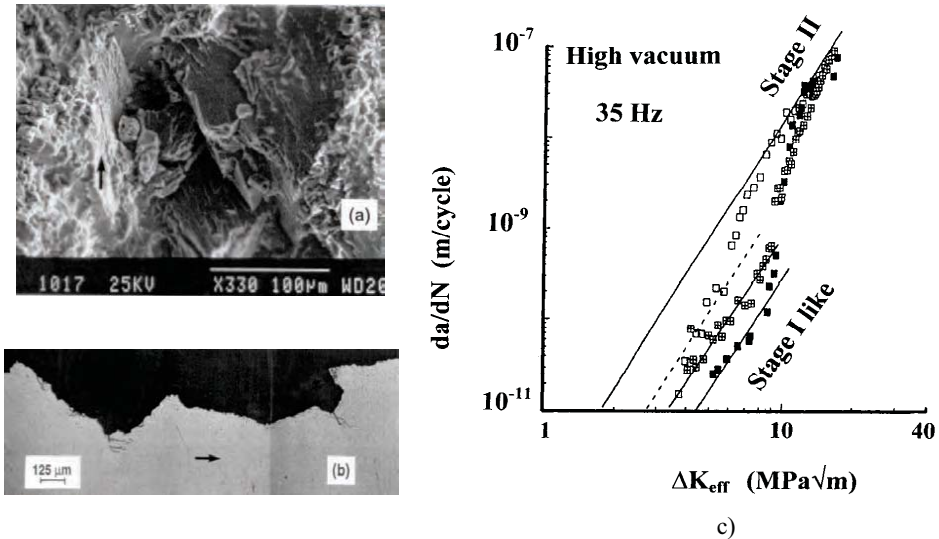


Fig. 13: Influence of microstructure on intrinsic stage I-like in Ti-6Al-4V: a) crystallographic crack surface; b) crack profile in bimodal microstructure; c) da/dN vs ΔK_{eff} (constant K_{max} , 35 Hz, 300°C, high vacuum) for three microstructures: equiaxed grain (open square), globular (windows) and lamellar (black square) [17].

Finally most of the differences observed in the intrinsic regime of cracks can be related to the transition between the different regimes and particularly to the enhanced retardation effect of microstructure in the near-threshold region for the crystallographic stage I-like regime. The intrinsic behavior of fatigue cracks, including naturally initiated micro-cracks, can be analyzed on such basis [9]. The framework corresponding to the three intrinsic propagation regimes can be used as a reference for analyzing environmentally assisted fatigue crack propagation.

Environmentally assisted effective fatigue crack propagation. Following the rationalization of intrinsic stage II propagation presented above, some similar rationalization of FCG in air would be expected after correction for crack closure and Young modulus effects. A compilation of stage II propagation data obtained in ambient air for a selection of alloys [5] is presented in Fig. 14.

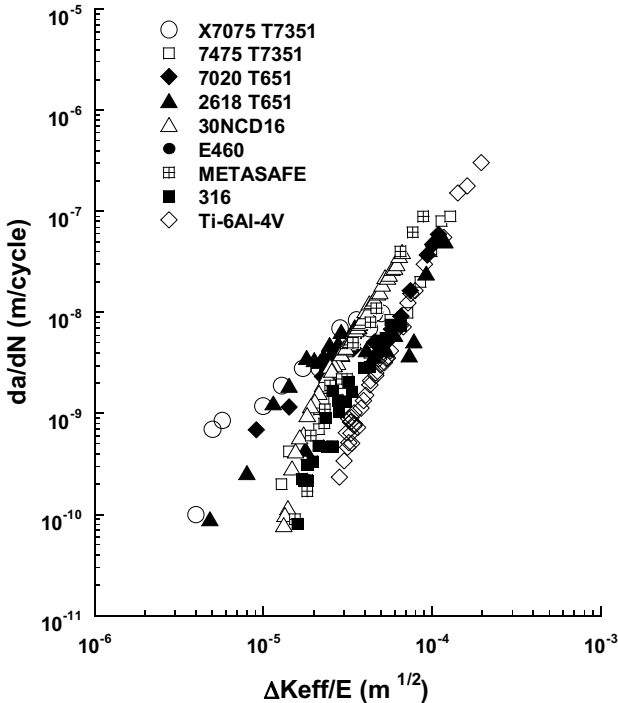


Fig. 14: Comparison of da/dN vs $\Delta K_{eff}/E$ crack growth data in air for various alloys [5].

Obviously there is no clear rationalization in air. The sensitivity to atmospheric environment is shown strongly dependent as well on base metals, addition elements, and microstructures (see 7075 alloy in three different conditions) as on R ratio and growth rate. However, a typical common critical rate range $(da/dN)_{cr}$ can be pointed at about 10^{-8} m/cycle (fig.15). This critical step is associated to stress intensity factor ranges at which the plastic zone size at the crack tip is of the same order as grain or sub-grain diameters. In addition it has been shown that, for growth rates lower than this critical range, crack propagation results from a step-by-step advance mechanism instead of a cycle-by-cycle progression as generally observed in the Paris regime in air [22]. Following Achter [23], $(da/dN)_{cr}$ is a critical rate for hydrogen assistance to crack propagation.

On the basis of a wide compilation of experimental data in air and inert gas containing traces of water vapor, obtained on similar Aluminum alloys, steels and Ti alloys than those tested in vacuum, a comprehensive model has been established by J. Petit et al. [5, 6, 23, 25, 26].

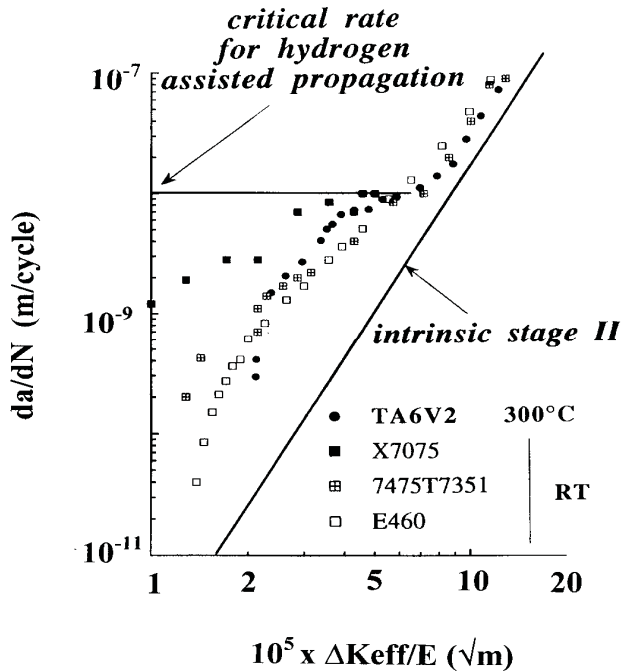


Fig. 15: Critical crack growth rate $(da/dN)_{cr}$ for hydrogen assistance in different alloys [5, 23, 24].

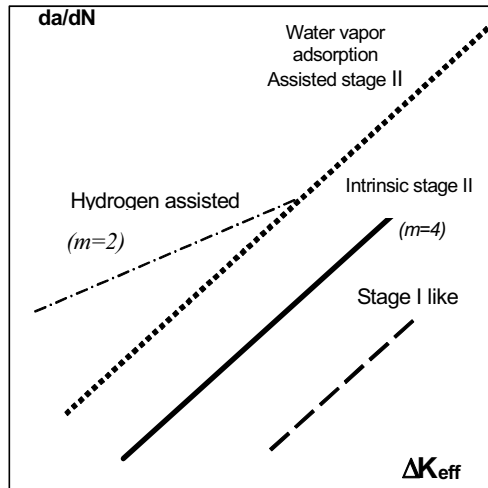


Fig. 16: schematic illustration of crack propagation regimes [25]

The crack growth behavior of metallic alloys in moist environment, including ambient air, has been described by mean of a two steps modeling for environmentally-assisted fatigue crack propagation superimposing two distinct processes as schematically illustrated in Fig. 16:

- i) Adsorption of water vapor molecules [5, 23, 24, 25, 26, 27, 28, 29, 30];
- ii) Hydrogen-assisted propagation in which hydrogen is provided by the dissociation of adsorbed water vapor molecules [5, 23, 24] as initially proposed by Wei et al. [31-33].

Adsorption assisted fatigue crack propagation. Adsorption is assumed, to diminish the cumulative critical displacement D^* , in a manner similar to that in which adsorption diminishes the energy required to create a new fresh unit surface [46].

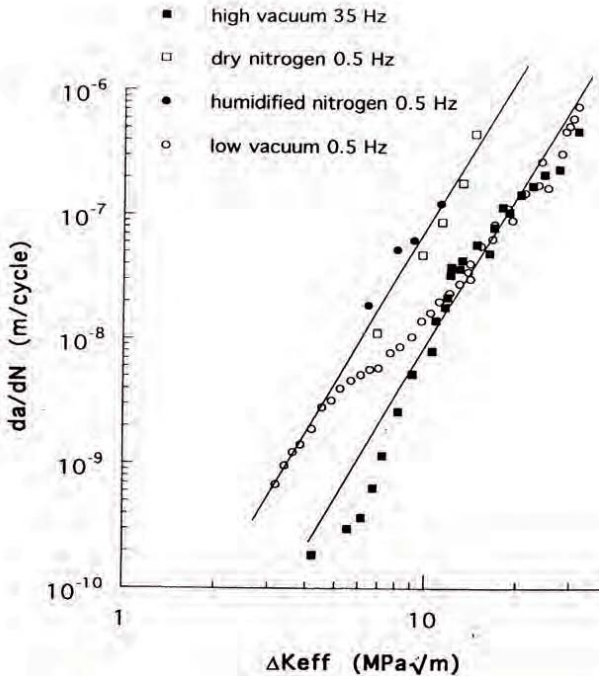


Figure 17: Adsorption assisted propagation in Ti-6Al-4V alloy as defined from tests at different frequencies and partial pressure of water vapor, compared to intrinsic crack propagation [5].

Thus D^* is assumed to depend on the adsorption coverage coefficient θ as defined by Langmuir (ref). At high frequencies, the growth increment is rapid to the extent that no significant adsorption can take place ($\theta = 0$ and $D^* = D_0$ as in vacuum). As the frequency decreases or/and da/dN decreases, more time becomes available for the molecules to form an adsorbed layer on the crack tip and thus the adsorption coverage increases ($0 < \theta < 1$) until reaching saturation ($\theta = 1$ and $D^* = D_{es}$) as in ambient air at conventional frequencies. Reconsidering the superposition model originally formulated by Wei [30], a revised formulation has been proposed in the form [5, 23]:

$$\left(\frac{da}{dN}\right)_e = \left(\frac{da}{dN}\right)_v + \theta \left[\left(\frac{da}{dN}\right)_{e,s} - \left(\frac{da}{dN}\right)_v \right] \quad (2)$$

with suffixes e = environmental, v = vacuum, e,s = saturated environmental effect, θ coverage coefficient of freshly created surfaces by adsorbed water vapor molecules as originally defined by Langmuir [50]. The variation of D^* with respect to θ can be written as follows:

$$1/D^* = (1/D^*_v + \theta (1/D^*_{e,s} - 1/D^*_v)) \quad (3)$$

where D^*_v is the intrinsic value of D^* for $\theta = 0$ and $D^*_{e,s}$ the saturated value of D^* when $\theta = 1$.

An illustration of adsorption assisted fatigue crack propagation is given in Fig. 17 for a Ti-6Al-4V alloy tested at 300°C in different gaseous atmosphere and different frequencies. Compared to the intrinsic propagation in high vacuum, the growth rate in dry nitrogen (15 ppm of water vapor) at low frequency (0.5Hz) or humidified nitrogen (1500ppm) at high frequency (35Hz) lead to the same adsorption assisted regime at saturation ($\theta = 1$). But in low vacuum (about 1 Pa) at low frequency (0.5Hz), a transitional behavior is observed, with the absence of environment influence for the higher growth rates, and a saturated effect of adsorption in the near threshold domain. A reassessment of Wei's model [31-33] has been done by G. Henaff et al [25] to describe the low rate range and to account for very low pressures. A critical point has been the formulation of the crack impedance for a quasi-stationary crack and a molecular flow.

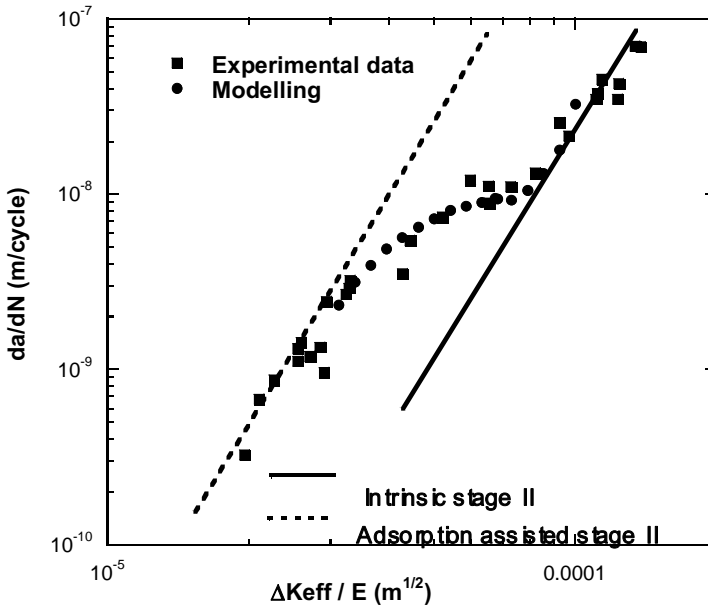


Fig. 18. Comparison of analytical modeling and experimental results for a 2022T851 Aluminum alloy tested in air at room temperature [26].

The S curve for the test in low vacuum of Figure 17 corresponds to θ evolutions as computed from the following equation:

$$\alpha S_0 \theta / 4F - \frac{1}{N_S V_a} \text{Log} (1 - \theta) = \frac{P_0}{4 N_0 RT} t \quad (4)$$

where α is the surface roughness parameter, V_a the average molecular rate, N_S number of stationary cycles.

The computations done on several other cases and materials reveal successful in accounting for the adsorption-assisted propagation [25]. C. Gasqueres et al. [26] have recently derived an analytical expression of the evolution of θ with respect to the exposure X to water vapor $P_0/2f$ (partial pressure P_0 and test frequency f) with an expression accounting for the influence of the area of new crack surface as follows:

$$\theta (X) = \{(X/3)^2 / ((X/3)^2 + 1)\}^2 \quad (5)$$

$$X = (P_{H_2O}/2f) \cdot \alpha [\Delta K_{eff}]^{-2} \quad (6)$$

An example of application of this model is presented in Fig. 18 with a comparison of the evolution of da/dN as given by experiments and by Equ. 2 using the analytical expression of θ (Equ.5 and 6), for a 2022T851 Aluminum alloy tested in air at room temperature [26].

Hydrogen assisted fatigue crack propagation. The occurrence of the Hydrogen assisted regime is associated with a typical change in the slope of the propagation curves which becomes close to 2:1 in most of the metallic alloys (Fig. 14, 15, 16). The transition from one regime to the other is marked by a more or less well defined plateau range. A propagation controlled by the $\Delta CTOD$ amplitude [37] with a theoretical slope of 2:1 provides a convenient description of the hydrogen assisted fatigue, and, using a superposition model [5], the following expression is considered for environment-assisted propagation:

$$da/dN = (da/dN)_{ad} + (da/dN)_H^2 \quad (7)$$

and finally:

$$da/dN = 1/D * (\Delta K_{eff}/\mu)^4 + [\Delta K_{eff}^2 - \Delta K_{eff,th}^2] / \mu \sigma \quad (8)$$

where σ is the yield stress of the material at the crack tip and $\Delta K_{eff,th}$ is the threshold value in the active environment. An example of application of the frame work for intrinsic and environmentally assisted propagation is given in figure 19 for a 7075T7351 Al alloy tested in air and vacuum.

Critical conditions for the occurrence of hydrogen-assisted propagation, which depends on Hydrogen concentration within the process zone at the crack tip, are as follows:

- Attainment of critical values of the parameters controlling the number of molecules of active species reaching the crack tip which lead to a sufficient partial pressure of water vapor to create an instantaneous adsorbed mono-layer; these parameters are the partial pressure in the surrounding of the specimen, the frequency, the growth rate and the R ratio. In such conditions, the mechanism can be considered as reaction-controlled as described by Wei et al. [31-33].

- Sufficiently low stress intensity factor in order to achieve a stationary crack and to localize the plastic deformation in a limited number of slip systems within a single grain (regardless of the grain size) at the crack tip ;

- Time long enough to allow Hydrogen to diffuse by dislocation dragging so as to attain a critical hydrogen concentration for metal embrittlement.

To explain the action of hydrogen, initially Beachem [34] proposed 'microscopic plasticity mechanisms' and 'severe, localized crack-tip deformations' to explain this behavior. Some authors have shown by in-situ observations that Hydrogen induces an easier motion of the dislocations and a subsequently earlier rupture as compared to vacuum [35, 36]. This is also consistent with Beachem's theory which suggests that instead Hydrogen locking dislocation in place, it unlocks them to multiply or move at reduced stresses' so that one might talk about enhanced plasticity. The exact controlling mechanisms are still in discussion.

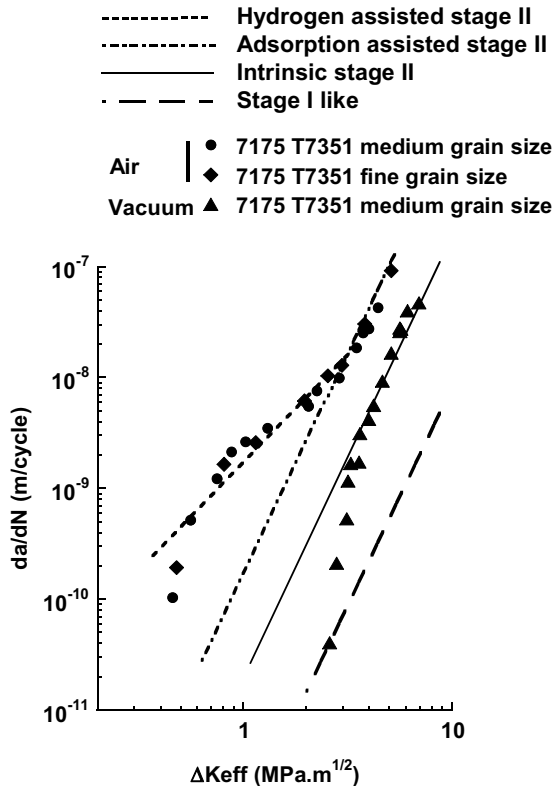


Fig. 19. Application of the modeling framework for intrinsic and environmentally assisted propagation to analyze crack propagation in air compared to high vacuum in a 7175 Al alloy.

Strain localization represents an alternative mechanism [38]. In accordance with this mechanism and on the basis of in-situ crack tip observations in air and in vacuum, and as mentioned above, McEvily and Gonzalez Vasquez [39] have proposed a representation of the influence of environment on the blunting process at the crack tip. The higher growth rates in air would result from a lesser blunting as compared to vacuum. This analysis is consistent with Davidson's and

Lankford's previous findings [40, 41]. According to these authors, as less energy is dissipated in plastic deformation in air, more energy is available for the growth process. It can be pointed out that the two approaches are not opposed. Finally it should be emphasized that further in-depth investigations covering different scientific fields, are still required in order to precisely define the Hydrogen assisted mechanism observed in humid atmospheres on metallic alloys.

Applications of the basic framework for crack propagation analysis.

Intrinsic propagation of small cracks. The intrinsic behavior of naturally initiated microcracks has been analyzed on the basis of the above framework with three intrinsic propagation regimes.

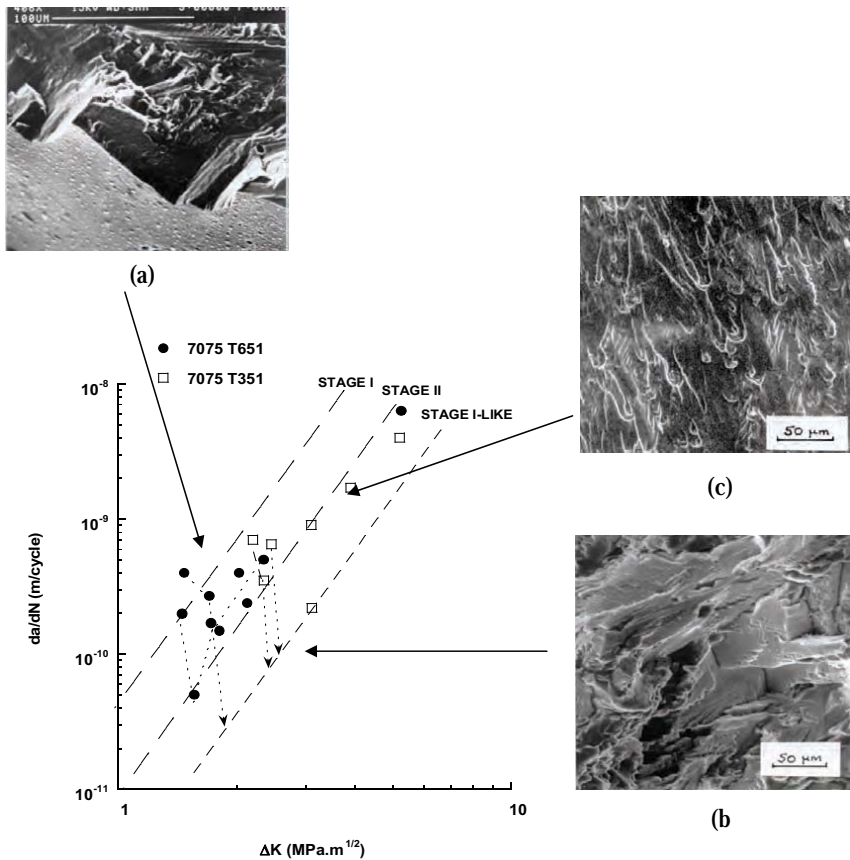


Fig. 20. Propagation data of naturally initiated microcracks grown in high vacuum in a 7075 alloy in different aged conditions (R=0.1, 35 Hz): comparison with the three intrinsic regimes.

An illustration is given in Fig. 20. As observed in Fig. 19a, a microcrack initiated at the surface of a specimen of a 7075 type alloy in T651 peak aged condition, grows in the stage I regime in the first grain. This is in accordance with the first description of a stage I crack by Forsyth [12]. Such

propagation is favored by GP and S' shareable precipitates which promote the localization of the deformation within PSB's [13, 15, 23]. When the crack has crossed one or more grain boundaries, the stage I-like propagation regime prevails giving highly retarded rates with a rough crystallographic surface morphology (Fig. 19b). For a larger crack extend and higher ΔK ranges, the propagation switches to the intermediate stage II regime (Fig. 19c). So, when the relation of the crack propagation with respect to the microstructure is well established, the LEFM concept, i.e. the ΔK concept, can be applied as well for short cracks as for long cracks after correction for closure and when condition for small scale yielding are fulfilled.

Influence of low temperature on crack path in a new generation 2024A T351 alloy. Aluminum alloys are widely used for constitutive parts of aircrafts and are consequently confronted to a wide range of temperature depending on altitude: from 300K (ambient temperature) on the ground down to 223K during a high altitude flight. A study of the Fatigue Crack Growth behavior in dry and cold air in comparison to ambient air at room temperature of new generation aluminum alloys has been carried out on an equipment specially designed and set up to achieve specimen cooling at 223K and to control the relative humidity (dew point of 223K) into the environmental chamber surrounding the tested specimen.

As illustrated in Fig. 21, the fatigue crack path in a naturally aged 2024A T351 alloy is strongly modified when the atmosphere is changed from laboratory air to cold and dry air at 223K. A highly crystallographic propagation mechanism is highlighted in the cold environment when a conventional stage II crack path is observed at room T.

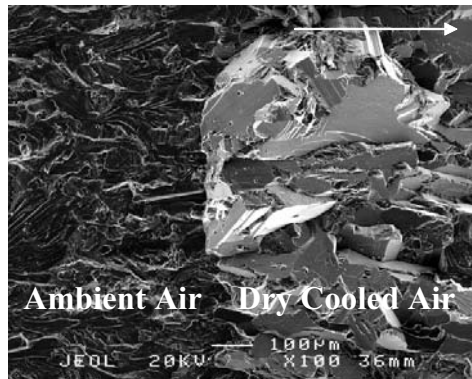


Fig. 21. Change in the fracture surface morphology of 2024A T351 alloy induced by dry cooled air.

The experimental data plotted in Fig. 22 from tests conducted in air and vacuum at room temperature and 223K show that the measured crack growth rates in cold air are substantially reduced in comparison with lab air and become comparable to that in vacuum which are not affected by the change of temperature. The higher resistance against crack propagation of the naturally aged temper in cold air as in vacuum is related to the underaged microstructure which promotes a localization of the deformation within a single slip system within each individual grain along the crack front, such localization being favored by the presence of fine shareable GP zones. The straight lines corresponding to the different regimes are directly extracted from the above presented modeling framework without any adjustable parameters. The crack propagation in air at

room T typically correspond to the intrinsic stage II regime at mid ΔK with a transition to the adsorption assisted regime in the near threshold domain. This material does not appear sensitive to hydrogen assistance.

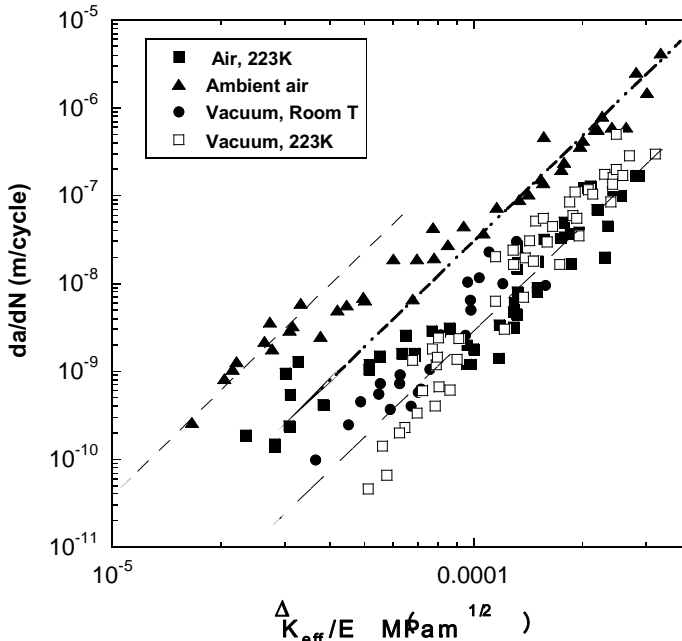
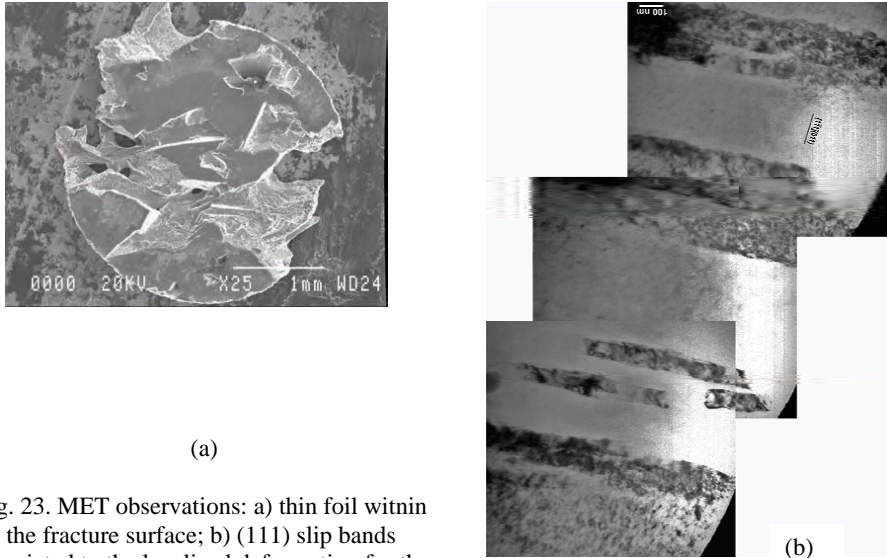


Fig. 22: Influence of low temperature (223K) as compared to ambient air on the crack propagation rate in a new generation 2024A alloy [26].

Finally, such crystallographic crack propagation mechanism prevailing in cold dry air and in high vacuum is in accordance with the intrinsic stage-I like regime with a typical fracture surface morphology as illustrated in Fig. 11a. However, it is noticeable that in the near threshold domain ($da/dN < 10^{-9}$ m/cycle), the crystallographic regime prevailing at 223K whatever the environment for the naturally aged alloys at higher growth rates (Fig. 22), switches to a much more flatter crack path and faster crack growth rates which becomes in accordance with the intrinsic stage II regime. Such a change may be related to an effect of the remaining 40 ppm of water vapor which could block slip reversibility by a few adsorbed water vapor molecules.

To go further in the analysis of the controlling mechanism of the crystallographic stage I like regime, TEM observations were performed on thin foils extracted within the fracture surface as illustrated in Fig. 23a. The profile of the foil corresponds to the zigzagging crack surface morphology, and TEM observations are only possible in the thin areas located in vicinity of hollows. An example is given in Fig. 23b which clearly shows dislocations located within (111) persistent slip bands. This observation is supporting a localization of the plastic deformation within a single slip system in each individual grain along the crack front at sufficiently low ΔK ranges.



(a)

(b)

Fig. 23. MET observations: a) thin foil within the fracture surface; b) (111) slip bands associated to the localized deformation for the Stage I like propagation [26].

Influence of environment on Ultra-Slow Crack Propagation in Al alloys. A study of the fatigue properties of lightweight materials has been undertaken by Stanzl-Tcshegg et al. [42- 44] in view of weight reduction and fuel saving for car industries.

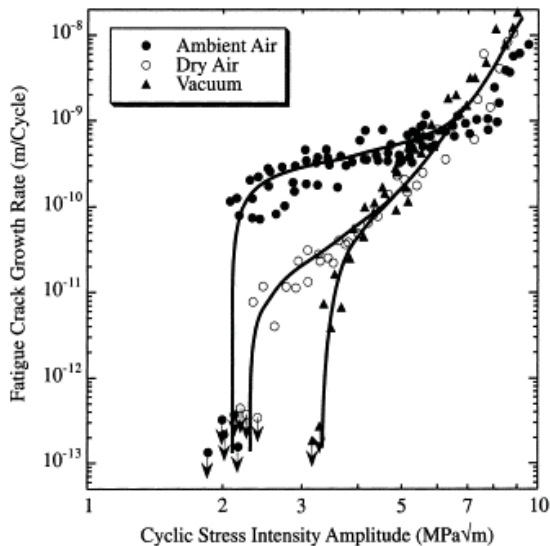


Figure 24: Fatigue crack growth rates for constant stress intensity cycling of 2024-T351 at ultrasonic frequency in ambient air (dots), dry air (circles) and in a vacuum (triangles) [44].

The fatigue properties of aluminum alloys are known to become worse when specimens are cycled in ambient air instead of vacuum as described above. In a first study [43] on a high strength aluminum alloy 2024T3, comparing crack growth and threshold behavior in humid air and dried air (Fig. 24), the authors concluded that water vapor in ambient air leads to hydrogen embrittlement responsible for the resulting higher growth rates and the lower threshold in comparison to vacuum. They assumed that the growth rates for conventional and ultrasonic testing are similar if the fatigue crack growth is slower than the diffusion process of hydrogen, i.e. some 10^{-9} m/cycle. This is in accordance with the above presented two steps modeling.

More recent results on 2024T3 and 7075T-UA and -OA alloys confirm the absence of influence of the test frequency on the threshold and on the crack growth rates when the effect of environment is saturated (as in ambient air at positive R ratio), or in high vacuum (no effect of environment). Between these two limiting cases, when the partial pressure of water vapor at the crack tip is reduced (as in air at a R ratio of -1 or in dry air), the growth rates at high frequency are reduced in the mid- ΔK range where a growth rate plateau range is typically observed in an active environment, which level depends on the exposure to water vapor (partial pressure of water vapor divided by the test frequency) [5, 25]. In conclusion, tests at very high frequency can give valuable information on the controlling mechanisms, and in the present case add weight to the two steps modeling.

Influence of environment on Ultra-Slow Crack Propagation in Ti-6Al-4V alloy. A comparison of fatigue-crack growth in Ti-6Al-4V at high frequencies of about 1 kHz and conventional frequencies in ambient temperature air and vacuum ($\sim 10^{-6}$ torr) is shown in Fig. 25 [45].

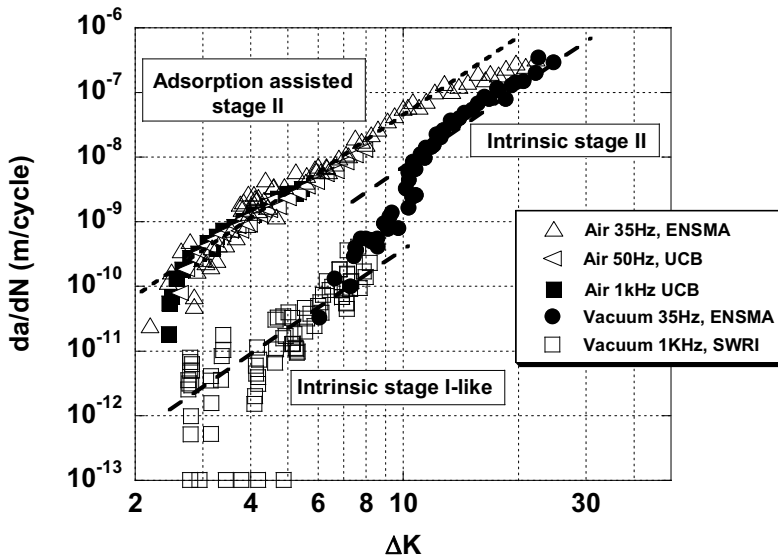


Figure 25: Influence of environment on crack propagation in Ti-6Al-4V alloy at 1 KHz [45] and conventional frequencies of 35 to 50Hz [17].

High frequency tests and tests at 50Hz were run at R ratios between 0.6 and 0.8 while tests at 35Hz were closure corrected. Hence all data can be considered as effective data. Although the threshold values are essentially unchanged ($\Delta K_{th} = 2.6 \text{ MPa}\sqrt{\text{m}}$ in air versus $2.7 \text{ MPa}\sqrt{\text{m}}$ in vacuum), crack growth rates are some two to three orders of magnitude faster in air than in vacuum. In the light of the two step fatigue crack propagation modeling described above, water vapor adsorption would be considered as the dominant phenomenon since it is very rapid and consistent with the absence of effect of frequency on crack growth rates in air between 20 and 20000 Hz. Hydrogen assistance has been shown operative at substantially higher temperatures as demonstrated at 300°C by Sarrazin-Baudoux et al. [17]. The highly retarded propagation in high vacuum can be analyzed as a combination of the effect of absence of environment assistance and of the effect of localization of the deformation within the basal slip system leading to a very rough crystallographic crack path when slip reversibility is facilitated by the absence of immediately adsorbed gas on the fresh crack surfaces. The critical exposure for the inhibition of slip reversibility has been shown to be about $10^{-2} \text{ Pa}\cdot\text{s}$ at 300°C for this alloy. In such condition, a stage I like propagation is developing with enhanced retardation induced by crack deviation and branching in addition to crack arrest at grain boundaries which act as microstructure barriers against slip propagation from one grain to neighbor grains [7, 17, 18].

Evaluation of propagation life in gigacycle fatigue. These examples on the influence of environment on ultra-slow fatigue crack growth compared to conventional high cycle fatigue in the near-threshold regime, underline the interest and the importance of exploring this domain by means of high frequency servo-hydraulic frames or ultrasonic equipments. Particularly, they demonstrate that ultra-slow fatigue crack propagation in high vacuum corresponds mainly to a highly retarded stage I like propagation, with a deformation localized within a single slip system in each grain. Comparison with tests in air shows that the influence of the test frequency is in accordance with the adsorption assisted propagation.

The ultraslow propagation existing in inert environmental condition in the near threshold condition has to be considered when a crack is growing in the bulk of an alloy as often observed in gigacycle fatigue [48]. In such condition, the estimation of the life for the propagation of a crack initiated, for example, on a fish eye in high strength steels must be done with a propagation law established in vacuum in the ultra slow regime. A first approach can be made using the intrinsic propagation law for a stage II crack in high strength steels which can be calculated from Equ.2 as:

$$da/dN = 7.7 \cdot 10^{-14} (\Delta K_{eff})^4 \quad (9)$$

At a given stress intensity factor amplitude, and neglecting possible effect of closure in a first approximation, the corresponding growth rates are about 100 times slower than that computed from data in air. In addition, a crystallographic regime would be retarded by another order of magnitude. Hence the estimation of the portion of life due to crack propagation could be greater of about two to three orders of magnitude than speculated from test in air.

Conclusion

Through a literature overview of the main progresses made during the last 30 years on the knowledge of basic mechanisms and mechanics of fatigue crack propagation in metallic alloys, and based on some recent works specifically dedicated to the identification and the modeling of the related governing mechanisms, some conclusions or comments can be drawn as follows:

1 – Most of the theoretical models developed since the initial works of Mc Clintock, Rice and Weertman do not take into account any potential influence of environment; so any pertinent correlation between such models and experiments should be done using data provided by

experiments conducted in inert environment. The estimation of the portion of life due to crack propagation in ultra high cycle fatigue is a typical example.

2 – Since Elber primary description of crack closure, the necessity of eliminating the closure contribution when one intends to determine the specific role of the effective driving force and to identify the corresponding mechanisms has been clearly demonstrated.

3 – Based on numerous experiments on metallic alloys, three intrinsic propagation regimes (i.e. in inert environment and with closure correction) have been clearly identified with respect to the microstructure:

i) Intrinsic stage I identified on single crystals, resulting from a shearing mechanism, also typical of the early propagation of surface microcracks in the first grains.

ii) Intrinsic stage II propagation observed on most of the metallic alloys in the mid ΔK range, with a crack path normal to the stress axis, which results from an alternative slip mechanism on two (or more) sets of symmetrical slip systems. A modeling has been derived as $da/dN = A/D^* \cdot (\Delta K_{eff}/E)^4$ for this regime poorly dependent on alloy composition, microstructure, yield strength and grain size.

ii) Intrinsic stage I-like propagation corresponds to a crystallographic mechanism associated to deformation localized within each individual grain along the crack front and highly sensitive to microstructure. The shielding effects on the stress intensity factor induced by crack branching, crack deviation and microstructural barriers (grain boundaries, matrix-precipitate interfaces...), induce highly retarded growth rates if compared to stage II.

4 – The environment effect in air at room temperature and moderate high or low temperatures is due to atmospheric water vapor. The concept of inert environment has to be carefully used specially at low growth rates or/and low frequencies; for example, inert gas like nitrogen, helium or argon containing traces of water vapor of the order of a few ppm, should not be considered as inert condition even at room temperature and specially in the near-threshold area.

5 – The crack propagation behavior in moist environment of metallic alloys including Al, Fe and Ti based alloys can be described by superimposing two distinct processes:

i) Adsorption of water vapor molecules which promotes the growth process without altering the basis intrinsic mechanism of damage accumulation. Adsorption of gaseous species onto fresh surfaces is analyzed as a decrease in the critical cumulated displacement D^* described in term of the surface coverage coefficient θ . This regime is generally operative in the mid rate range at atmospheric pressure, and can be active near-threshold condition at sufficiently low pressure or/and by lowering the test frequency. Low temperature experiments on a 2024A T351 alloy give a nice illustration of this regime.

ii) Hydrogen-assisted propagation as initially described by Wei and co-authors, in which hydrogen is provided by the dissociation of adsorbed water vapor, leads to the fastest propagation. Critical conditions for such process would thus correspond with the kinetics of the reaction and its dependence on parameters as water vapor pressure, time (frequency) and temperature. This regime is generally observed in near-threshold conditions, at growth rate below a critical step ranging about 10^{-8} m/cycle which corresponds to stress intensity factor ranges at which the plastic deformation becomes localized within each individual grain along the crack front.

7- The behavior of short crack can be basically analyzed with respect to the microstructure by mean of the different propagation regimes of the proposed framework, when conditions for LEFM application are fulfilled. A typical illustration is given for naturally initiated small cracks in an Al alloy.

References

- [1] J. Bäcklund, A.F. Blom and C.J. Beevers, *Fatigue thresholds, Fundamentals and Engineering Applications*, EMAS pub.,(1981).
- [2] D. Davidson and S. Suresh, *Fatigue crack growth threshold concept*, TMS AIME Pub., Warrendale, Pensylvanie, USA., (1984).
- [3] J.C. Newman Jr. and R.S. Piascik, *Fatigue Crack Growth Thresholds, Endurance Limits and Design*, (2000) ASTM STP 1372
- [4] J.C. Newman, Jr. and W. Elber, *Mechanics of Fatigue Crack Closure*, ASTM STP 982, American Society for Testing and Materials Pub., Philadelphia, USA, (1988).
- [5] J. Petit J., G. Hénaff and C. Sarrazin-Baudoux in *Fatigue Crack Growth Threshold, Endurance Limits and Design, ASTM STP 1372*, Newman Jr. J. C. and Piascik R. S. Eds. American Society for Testing and Materials, Philadelphia, Pa, USA, (2000), p. 3.
- [6] J. Petit, G. Hénaff and C. Sarrazin-Baudoux, in, *Comprehensive Structural Integrity*, Volume 6, *Environmentally-assisted Fracture*, J. Petit and P. Scott eds., (2003), p. 211.
- [7] K.J. Miller and E.R. de los Rios, *Short Fatigue Cracks*, ESIS 13, Mechanical Engineering Pub. Ltd., London, UK, (1992).
- [8] J. Lankford and R.O. Ritchie, *Small Fatigue Cracks*, TMS AIME Pub., Warrendale, USA, (1986).
- [9] J. Petit, in: “Small fatigue cracks : mechanics and mechanisms”, Ed. K. S. Ravichandran, R. O. Ritchie and Y. Murakami, Engineering Foundation pub., 1999, p. 167.
- [10] E. R. De Los Rios, H. J. Mohamed, and K.J. Miller, *Fatigue & fracture of Engineering Materials and Structures*, vol. 8., (1985), p. 49.
- [11] H. J. Gudladt, and J.Petit, , *Scripta Metall. & Mater.*, n° 25, (1991), p. 2507
- [12] J.P.E. Forsyth, in: *Crack propagation*, Proceedings of Crankfield Symposium, London, Her Majesty’s Stationery Office (1962), p. 76
- [13] Petit, J., in: *Theoretical and numerical analysis of fatigue*, A. F. Blom and C. J. Beevers eds., EMAS Pub., London, (1992), p. 131.
- [14] Petit, J., and Kosche, K., in: *Short Fatigue Cracks*, ESIS 13, K.J. Miller and E.R. de los Rios eds, ESIS 13, Mechanical Engineering Pub. Ltd., London, UK, (1992), p.135
- [15] R.J.Selines, Ph D Thesis, MIT, USA., (1971).
- [16] Starke, Jr., E.A., Lin, F.S., Chen, R.T. and Heikkinen, H.C., in: *Fatigue crack growth Threshold concepts*, edited by Davidson, D. and Suresh, S., TMS AIME pub., (1984), p. 43.
- [17] C. Sarrazin-Baudoux, S. Lesterlin, and J. Petit, in: *ASTM-STP 1297*, American Society for Testing and Materials Pub., Philadelphia, USA, (1996), p.117.
- [18] S. Suresh, *Metallurgical Transactions.*, 16A, (1985), p. 249.
- [19] J. R.Rice, *International Conf. on Fracture*, Sendai, Japan, (1965), p. 283.
- [20] J. Weertman, *Internat. Journal of Fracture Mechanics* , 2, (1966), p. 460.
- [21] J. Petit, J. and G. Hénaff, *Scripta Metallurgica* , 25, (1991), p. 2683.
- [22] D. L. Davidson, and J. Lankford, *Int. Journal of Fracture*, 17, (1981), p. 257.

- [23] J. Petit, J., in: Fatigue Crack growth Thresholds Concepts, D. Davidson, and S. Suresh eds, TMS AIME pub., (1983), p. 3.
- [24] M. R. Achter, Scripta Metallurgica, n° 2, (1968), p. 525.
- [25] G. Henaff, K. Marchal, and J. Petit, Acta Metallurgica et Materialia, 43, (1995), p. 2931.
- [26] C. Gasqueres, C. Sarrazin-Baudoux and J. Petit Fatigue in: proc. FCP 2006, A. Carpintieri ed. ,Parma, Italy (2006) in press.
- [27] I. Langmuir, Journal of the American Chemical Society, 40, (1918), p. 1361.
- [28] F. J. Bradshaw, Scripta Metallurgica, 1, (1967), p. 41.
- [29] S. P. Lynch, Acta Metallurgica , 36, (1988), p.2639.
- [30] B. Bouchet, J. de Fouquet, M. Aguilon, Acta Metallurgica 23, (1976), p.1325.
- [31] R. P. Wei, ASTM STP 675, ASTM pub., (1979), p.816.
- [32] R. P. Wei, and G. W. Simmons, International Journal of Fatigue, 17, (1981), p.235.
- [33] P.S. Pao, M. Gao, and R.P. Wei, in ASTM-STP 924, edited by R.P. Wei and R.P. Gangloff, American Society for Testing and Materials Pub., Philadelphia, USA, (1988) p. 182.
- [34] D. Beachem, Metall Trans, 3 (1972), p. 437.
- [35] T. Tabata and H. K. Birnbaum, Scripta Metall., 17 (1984), p. 947.
- [36] H. K. Birnbaum and P. Sofronis, Mater. Sci. and Engng. 176 A (1994), p. 191.
- [37] F. A. McClintock, *Proc. Fracture of Solids*, Maple Valley WA, (1963), pp. 65-102.
- [38] Louthan, M.R., Jr. , Scripta Met. , 17, (1983), p. 451.
- [39] Mc Evily, A.J. and Gonzalez Velasquez, J.L., Met. Trans., 23A, (1992), p.2211.
- [40] D.L. Davidson, Fat. Engng. Mat. Struct., 3, (1983), p. 229.
- [41] D.L. Davidson, and J.L. Lankford, Fat. Engng. Mat. Struct., 6, (1983), p. 241.
- [42] S. E. Stanzl-Tschegg and H. Mayer, *Int. Jal of Fatigue*, 23 (2001), p. S221
- [43] B. Holper, H. Mayer, A. K. Vasudevan and S. E. Stanzl-Tschegg, International Journal of Fatigue, 25 (2003), p. 397
- [44] B. Holper, H. Mayer, A. K. Vasudevan and S. E. Stanzl-Tschegg, Int. Journal of Fatigue, 26 (2004), p. 27.
- [45] R. O. Ritchie, D. L. Davidson, B. L. Boyce, J. P. Campbell and O. Roder, Fatigue Fract Eng Mater Struct., 22 (1999), p. 621
- [46] S. Suresh, Metall. Trans., 16A (1985), p. 249.
- [47] K. J. Miller and E. R. De Los Rios, *The Behaviour of Short Fatigue Cracks*, Mechanical Engineering Publications Limited, London, U.-K. (1986).
- [48] C. Bathias, Fat. Fract. Engng. Mater. Struct., 22 (1999), p.559.